Small and Medium Rings, 75[1)]

Syntheses, Photoelectron Spectra, and Photoreactivity of Polycyclic 1,5-Diketones: Transannular Interaction in the Cyclooctane-1,5-dione Fragment

Bernhard Albert[a], Dominik Elsässer[a], Dieter Heckel[a], Siglinde Kopmeier[a], Hans-Dieter Martin*[a], Bernhard Mayer[a], Tahsin J. Chow*[bc], Tung-Kung Wu[c], and Show-Kei Yeh[b]

Institut für Organische Chemie und Makromolekulare Chemie der Universität Düsseldorf[a], Universitätsstraße 1, D-4000 Düsseldorf 1, F.R.G.

Institute of Chemistry, Academia Sinica[b], Nankang, Taipei, Taiwan, Republic of China

Department of Chemistry, National Taiwan University[c], Taipei, Taiwan, Republic of China

Received August 13, 1990

Key Words: PE spectroscopy / Lone-pair interaction / Orbitals, localized / Orbitals, precanonical / 1,5-Diketones, polycyclic

Five polycyclic 1,5-diketones **1**–**4** and **6** are synthesized and studied by means of He(I_α) PE spectroscopy. Comparison of the spectra indicates significant differences in Orbital Interaction Through Bond, which is explained by computational methods, especially by analyses of the precanonical MOs. The lone pair splitting observed in diketone **1**, $\Delta I(n)$ = 0.75 eV, seems to be the largest one ever found in a 1,5-diketone, obviously due to a favourable zigzag topology of the σ frame. In addition, coupling reactions and photoreactivity are studied in compound **6**, which seemed to be well suited for Orbital Interaction Through Space. The crystal structure of **6** and its photoproduct **21** is solved by X-ray crystallography.

Transannular (orbital) interaction of functional groups in polychromophoric systems may be discussed within the frame of models as either being effective directly, "through space", or indirectly transmitted by a σ-skeleton, "through bond"[2)]. He(I_α) PE spectroscopy has proved to be an excellent instrument to analyze these interactions, since, assuming validity of Koopmans' theorem[3)], the experimental ionization energies I_m can be assigned to the orbital energies ε_i of the corresponding molecule. Thus, observable energetic splits in the PE spectra often reveal energetic differences of formerly degenerate molecular orbitals and, as a consequence, can serve as an experimental measure for the magnitude of transannular interaction.

It is obvious that especially Orbital Interaction Through Bond (OITB) depends strongly on the nature of the transmitting σ framework of a molecule. In order to study this influence of structural details on the magnitude of orbital interaction, molecules with a comparable and defined geometry are required.

Recently we became aware of the fact that even the color of polyketones is strongly affected by the shape of the intervening σ system[4)]. Since the underlying topology in these cases is that of a 1,5-dioxo moiety we designed a series of 1,5-diketones with a well defined, experimentally unambigous structure. Moreover, it was required that all studied compounds exhibit symmetry-equivalent carbonyl groups in order to facilitate an analysis by PE spectroscopy.

Compounds **1**–**6** prove to be very useful for that purpose. They all contain a common structural element: The cyclooctane-1,5-dione moiety which fixes the orientation of the carbonyl chromophores and thus determines the individual pathway of transmission for Orbital Interaction Through Bond. In the present communication we report on the syntheses of these compounds, their PE spectra and structural analyses by X-ray, force-field, and semiempirical techniques. Detailed analysis by computational methods will help to discuss the experimental spectra. In addition, coupling reactions and photochemical experiments will reveal electronic properties of cage compound **6**, where the almost parallel alignment of the very close carbonyl groups seems to be well suited for Orbital Interaction Through Space (OITS).

Scheme 1

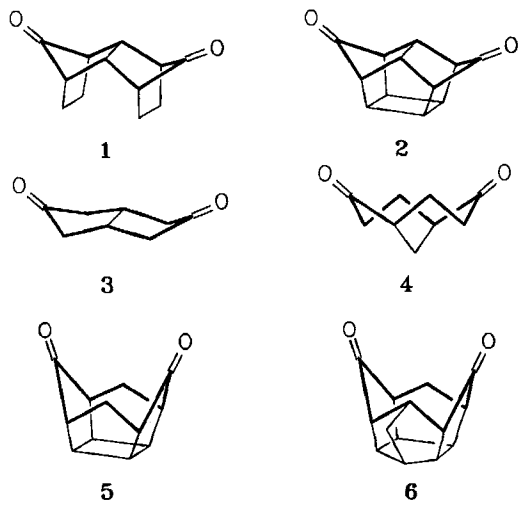

 © VCH Verlagsgesellschaft mbH, D-6940 Weinheim, 1991 0009–2940/91/0404–0803 $ 3.50+.25/0

PE Spectroscopy

The He(I_α) PE spectra of **1**–**4** and **6** are illustrated in Figure 1[5]. Experimental ionization energies I_m and calculated orbital energies ε_i are listed in Table 1.

Although all compounds contain the same cyclooctane-1,5-dione moiety as structural element the spectra of these five diketones exhibit significant differences. The most remarkable of them refer to the observed energetic split of the

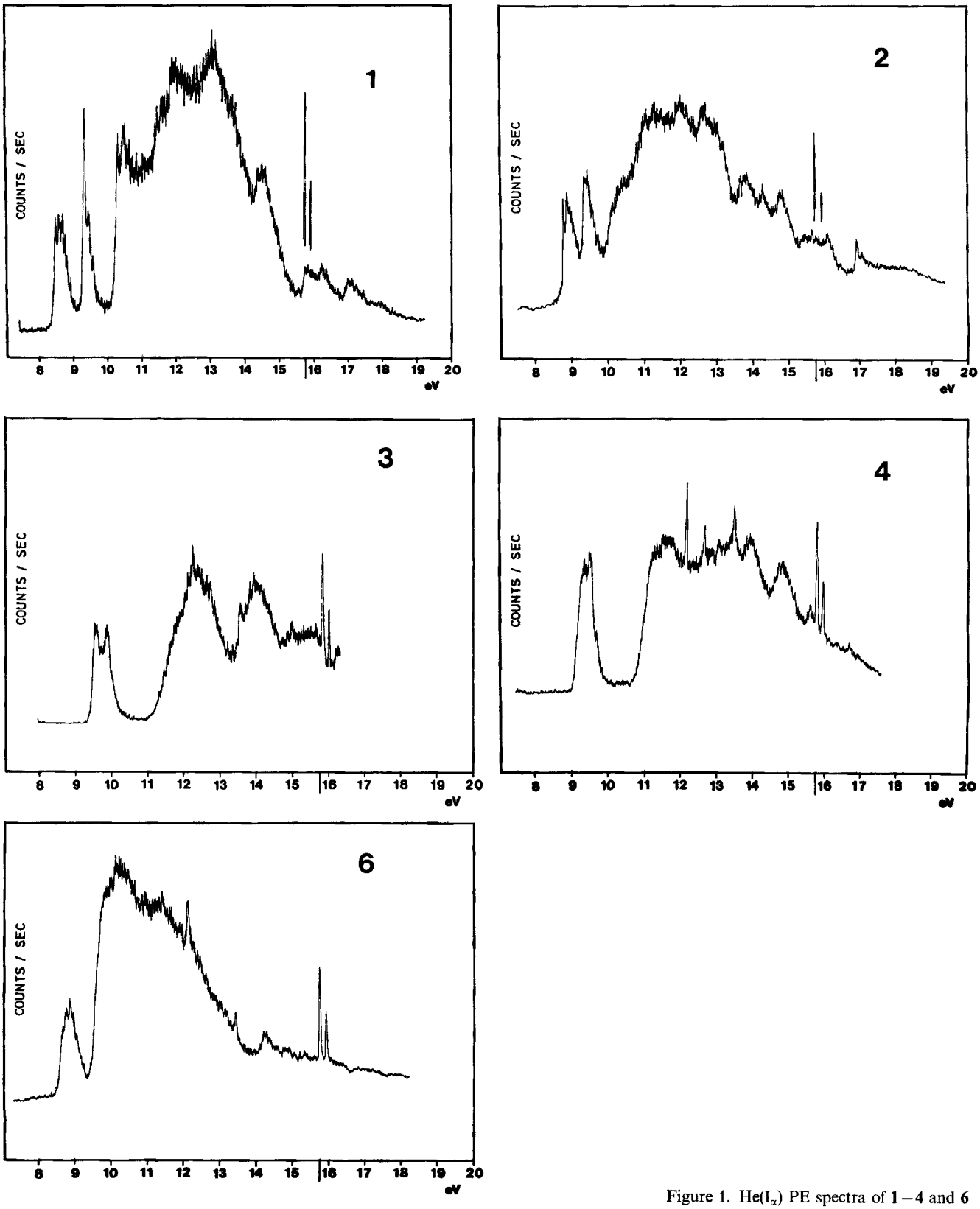

Figure 1. He(I_α) PE spectra of **1**–**4** and **6**

Table 1. Experimental n-ionization energies and calculated energies of **1**–**6**

Compound		MNDO $-\epsilon_i$/eV	HAM/3 $-\epsilon_i$/eV	STO-3G $-\epsilon_i$/eV	Exp. I_m/eV	
	$-\epsilon_1$	10.27	8.87	7.76	8.65	$I_{m,1}$
1	$-\epsilon_2$	10.64	9.18	8.51	9.40	$I_{m,2}$
	$\Delta\epsilon$	0.37	0.31	0.75	0.75	ΔI_m
	$-\epsilon_1$	10.46	9.38	8.06	8.90	$I_{m,1}$
2	$-\epsilon_2$	10.71	9.53	8.59	9.35	$I_{m,2}$
	$\Delta\epsilon$	0.25	0.15	0.53	0.45	ΔI_m
	$-\epsilon_1$	10.71	9.18	8.41	9.45	$I_{m,1}$
3	$-\epsilon_2$	10.93	9.29	8.93	9.80	$I_{m,2}$
	$\Delta\epsilon$	0.22	0.11	0.52	0.35	ΔI_m
	$-\epsilon_1$	10.74	9.35	8.46	9.33	$I_{m,1}$
4	$-\epsilon_2$	10.84	9.38	8.57	9.48	$I_{m,2}$
	$\Delta\epsilon$	0.07	0.03	0.11	0.15	ΔI_m
	$-\epsilon_1$	10.60	9.19	8.34		$I_{m,1}$
5	$-\epsilon_2$	10.75	9.37	8.57		$I_{m,2}$
	$\Delta\epsilon$	0.15	0.18	0.11		Δ_m
	$-\epsilon_1$	10.54	9.12	8.32	8.8–	$I_{m,1}$
6	$-\epsilon_2$	10.73	9.23	8.57	8.90	$I_{m,2}$
	$\Delta\epsilon$	0.19	0.11	0.25	<0.1	ΔI_m

first two bands which varies from a maximum of 0.75 eV (**1**) to an unexpected minimum of nearly 0 eV (**6**). Assuming validity of Koopmans' theorem[3] the first two ionization energies can be assigned to the orbital energies of the HOMO- and SHOMO combination of the oxygen lone pairs. Thus, the surprising variety of the recorded energetic splits reveals a remarkable sensitivity of orbital interaction towards structural details in the σ framework (cf. Discussion).

Syntheses

Syntheses of bicyclo[3.3.0]octane-3,7-dione (**3**)[6] and bicyclo[3.3.1]nonane-2,6-dione (**4**)[7] have previously been described. Hexacyclotetradecanedione **6** has been prepared recently from a cage dimer of norbornadiene[8,9] by cutting open the parent hydrocarbon **7**.

Scheme 2

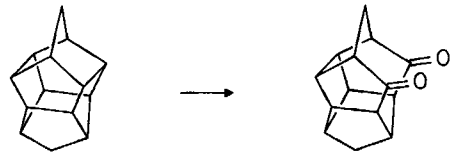

7 **6**

The saturated isodrine derivative **1** and its birdcage analog **2** were synthesized as depicted in Scheme 3, both starting with the well-known Diels-Alder adduct **8**[10]. Cage diketone **2** was prepared according to known procedures[11,12], and the new isodrine diketone **1** was obtained by a similar synthetic strategy: Reductive cleavage of ester **8** and subsequent catalytic reduction gives the partially saturated alcohol **10**, which is dehalogenated and reduced again to give the fully saturated intermediate **12** according to the diimine method[13]. Finally, conversion into the diketone **1** is accomplished by common methods of oxidation and deketalization.

Scheme 3

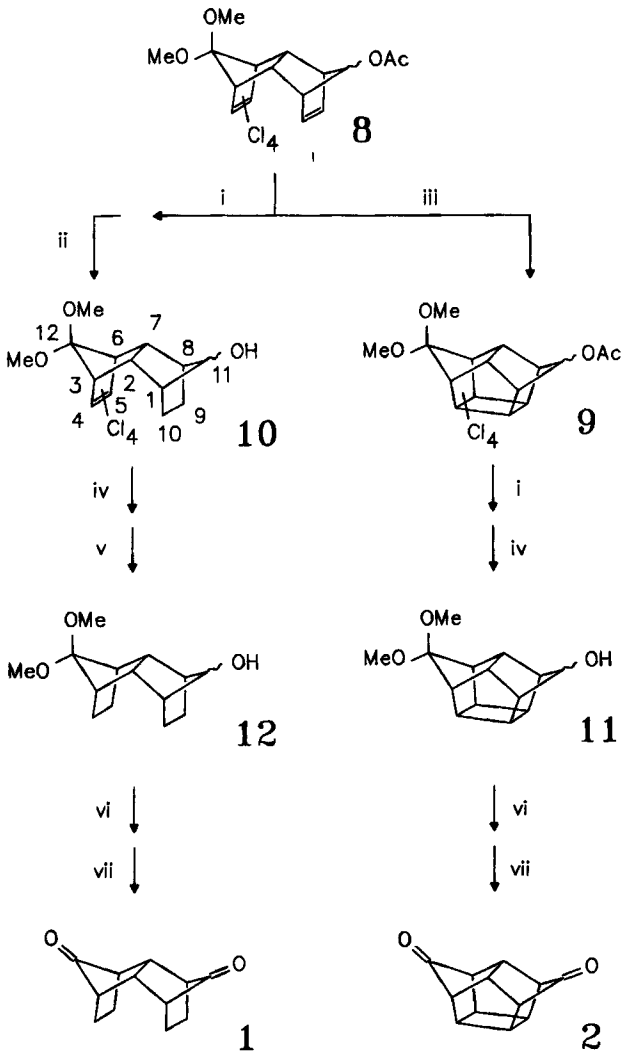

i) $LiAlH_4$; THF. ii) H_2; Pd-C. iii) *hν*; acetone / ethyl acetate 1:9. iv) Na; NH_3(liq.). v) $N_2H_4 \cdot H_2O$; $CuSO_4$; H_2O_2 (30%). vi) PCC; CH_2Cl_2. vii) 6 M $HClO_4$.

Coupling Reactions

When diketone **6** is treated with zinc in acetic acid[14], diol **13** is formed in nearly quantitative yield[15].

The formerly observed pinacolization of [4]peristylanedione **5** may be compared with the ring closure reaction of **6**. When **5** was treated with zink in ether saturated with dry

hydrogen chloride, diol **14** was formed in 74% yield[5b]. The structural similarity of **5** and **6** is obvious.

Scheme 4

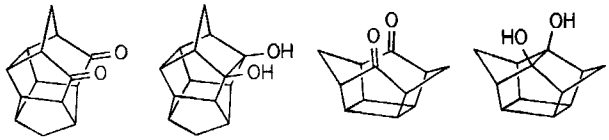

6 **13** **5** **14**

Photochemical Reactions of 6

Photolysis of **6** was carried out in a quartz vessel containing 2-propanol as solvent by irradiation with a medium-pressure mercury lamp for 30 minutes, and diol **13** was collected afterwards in quantitative yield[15].

The presence of an oxa radical intermediate in the photolysis of **6** (cf. Discussion) can better be evidenced by performing the reaction in tetrahydrofuran[15]. Upon hydrogen abstraction by the excited state molecule of **6**, a THF radical is produced, which either can couple with the oxa radical of **6** to give the mono- THF adduct **15**, or couples with another excited **6** to give the bis-THF adduct **16**. The yield of **16** in this reaction is substantial (ca. 20%), indicating the high stability of the radicals derived from both THF and **6**. Compound **17** is formed by rearrangement of the original mono- THF adduct in the work-up procedures and may also be produced by partial hydrolysis of **16**. Complete hydrolyses of either **16** or **17** in acidic media yields **13** quantitatively.

Scheme 5

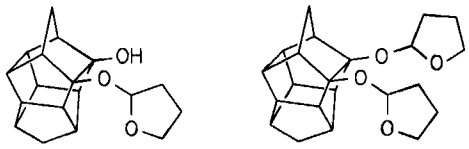

15 **16**

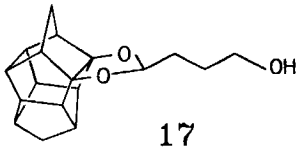

17

Analogous coupling reactions have been reported previously for a variety of compounds containing the cyclooctane-1,5-dione moiety[16]. For example, photolysis of **18** produces **19** in quantitative yield. The orbital arrangements in **18** are also similar to those in **6**. Presumably **18** is more flexible than **6**, but the alignments of the C=O groups in favor of the coupling reaction are very much alike. It should be noted that analogous intermolecular reactions are also commonly observed. However, the efficiency of intramolecular reactions must have been strongly enhanced by the proper alignment of orbitals within the molecules[17].

Scheme 6

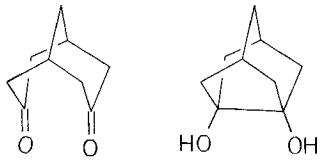

18 **19**

The photochemical reaction of **6** in the presence of benzophenone proceeds very differently as shown in the following example. A benzene solution of **6** containing benzophenone was irradiated with UV light for 14 hours. The major product isolated afterwards shows resonance lines of aromatic hydrogens in its ^{1}H-NMR spectrum (δ = 7.1–7.3, 5H). In the ^{13}C-NMR spectrum there are 18 distinct signals observed (2 secondary, 12 tertiary, and 4 quaternary carbon atoms), four of them in the aromatic region (3 tertiary and 1 quaternary carbon) and two for the carbonyl groups (δ = 221.7 and 222.8). These informations along with the molecular ion (m/z = 290 [M^+]) observed in the mass spectrum indicate that the product is derived from an oxidative coupling between **6** and a molecule of benzene. The position of the phenyl substituent could not be assigned readily, but was finally resolved by X-ray crystallography. A SCHAKAL drawing of the product **21** is shown in Figure 2. The phenyl group is attached to C(3), β to the carbonyl group. The formation of **21** apparently has not proceeded through the excited-state molecule of **6**. In this reaction benzophenone is the absorbing chromophore. It abstracts a hydrogen from **6** to generate a tertiary carbon radical which is trapped by benzene. Subsequent aromatization of the radical intermediate produces the adduct **21**. The carbonyl functionality of **6** does not seem to be involved in this photoreaction, since the same type of reactions is observed in the absence of carbonyl groups. For example, irradiation of the octaquinane **7** in the same way produces the phenyl adduct **20**. The regioselectivity of this reaction is analogous to the oxidation of **7** in acidic medium as previously described[8].

Scheme 7

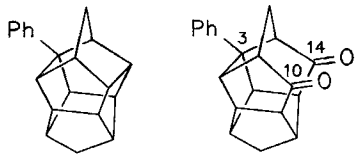

20 **21**

Crystal Structures of 6 and 21

Structure of 6

During the ring-opening process leading from **7**[8] to **6** a substantial amount of angle strain (from 94.6 to 102.3°) is released for angle C(11)–C(12)–C(13) (cf. Figure 3), and a relatively low-strain cyclooctanedione moiety is generated with the two carbonyl groups located at the 1,5-positions.

The crystal geometry of **6** is examined by X-ray diffraction analysis. The resulting atomic coordinates and thermal parameters for non-hydrogen atoms are listed in Table 2, and a SCHAKAL drawing of **6** is shown in Figure 3. The distance between the carbonyl is found to be 2.88 Å, and that between the oxygens is 3.46 Å. A directional angle of ca. 27° is found between the two carbonyl groups. Selected bond lengths and angles are listed in Tables 3 and 4.

Structure of 21

According to an X-ray diffraction analysis the crystal of **21** contains a pair of enantiomers and belongs to the orthorhombic space group $Pbc2_1$. The atomic coordinates and thermal parameters for non-hydrogen atoms are listed in Table 5. The directional angle between the C=O groups of **21** (31°) is a little larger than that of **6** (27°). As a consequence, the corresponding distances between the carbonyl carbon atoms (2.91 Å) as well as that between the oxygen atoms (3.57 Å) are also larger than those of **6**. The introduction of a phenyl substituent in **21** has broken down the symmetrical geometry of **6**. The variations in bond lengths and angles thus introduced to the cage skeleton are compared in Tables 3 and 4.

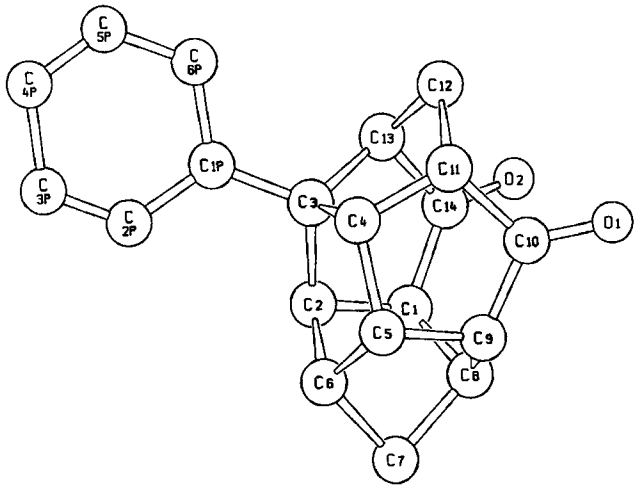

Figure 2. SCHAKAL drawing for the crystal structure of **21**

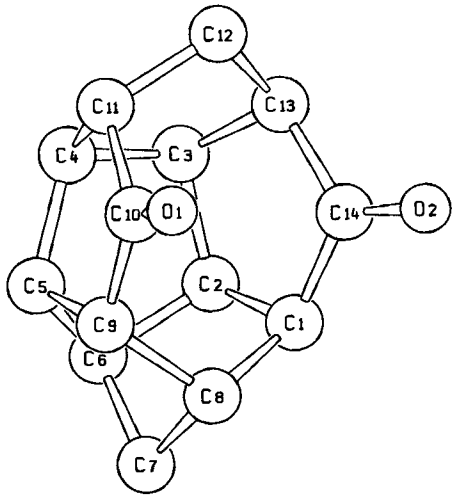

Figure 3. SCHAKAL drawing for the crystal structure of **6**

Table 2. Atomic coordinates and thermal parameters for non-hydrogen atoms of **6**. Estimated standard deviation to the last digit printed

Atoms	X	Y	Z	B(iso),Å²
O(1)	0.90527	0.11054	0.51027	4.22
O(2)	0.90540	-0.08942	0.31641	4.06
C(1)	1.20511	0.00749	0.26508	2.78
C(2)	1.42581	-0.01187	0.29747	2.80
C(3)	1.41628	-0.07047	0.40693	2.82
C(4)	1.41540	0.01924	0.49409	2.85
C(5)	1.42545	0.12611	0.43103	2.90
C(6)	1.50511	0.10237	0.31660	3.18
C(7)	1.37364	0.17239	0.24344	3.51
C(8)	1.17494	0.12877	0.28852	2.94
C(9)	1.20444	0.15693	0.41020	2.78
C(10)	1.08113	0.09552	0.49165	2.85
C(11)	1.21036	0.01210	0.54940	2.91
C(12)	1.13379	-0.10248	0.52940	3.24
C(13)	1.21193	-0.12603	0.41516	2.90
C(14)	1.08192	-0.07129	0.33005	2.76

Table 3. Selected bond lengths [Å] of **6** and **21** with standard deviations in parentheses

	6[a]	**21**[b]
C1-C8, C8-C9	1.554(2)	1.52(3), 1.56(4)
C1-C14, C9-C10	1.510(1)	1.52(3), 1.53(4)
C10-C11, C13-C14	1.527(1)	1.53(4), 1.54(4)
C11-C12, C12-C13	1.535(1)	1.54(3), 1.51(3)
C10-O1, C14-O2	1.213(2)	1.21(2), 1.22(2)

[a] Symmetrical bond lengths are averaged. — [b] Values are averaged for enantiomers.

Discussion of the PE Spectra

In Figure 1 the He(I_α) spectra exhibit a decreasing split of the HOMO and SHOMO energies in the sequence **1**–**4** and **6**. Both energies represent an n_+ or n_- combination of the formerly degenerate carbonyl lone pairs. All six model compounds have a cyclooctane ring in common, and the n-orbitals in all cases are separated by for σ bonds. Thus the transannular interaction can be classified as a 1,7-n,n-OITB.

Distances which help to point out the structural differences between **1**–**6** are given in Table 6.

Scheme 8

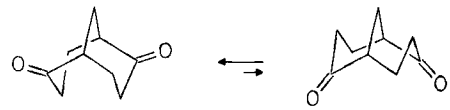

4a **4b**

Table 4. Selected bond angles [deg] of **6** and **21** with standard deviations in parentheses

Angles	6[a)]	21[b)]
C1-C2-C3,C4-C5-C6	105.0(1)	104.9(17), 104.8(16)
C1-C2-C6,C6-C5-C9	103.0(1)	101.6(17), 104.0(21)
C1-C8-C7,C7-C8-C9	99.3(1)	98.4(13), 98.1(15)
C1-C8-C9	112.5(1)	113.3(23)
C1-C14-C13,C9-C10-C11	110.3(1)	110.8(16), 108.7(15)
C2-C1-C8,C5-C9-C8	103.1(1)	105.6(12), 103.3(14)
C2-C1-C14,C5-C9-C10	106.4(1)	106.6(24), 107.6(25).
C2-C3-C4,C3-C4-C5	105.6(1)	105.7(19), 106.4(22)
C2-C3-C13,C5-C4-C11	108.1(1)	106.8(19), 107.5(18)
C2-C6-C5	101.5(1)	102.9(19)
C2-C6-C7,C5-C6-C7	103.7(1)	103.0(18), 103.6(16)
C3-C2-C6,C4-C5-C6	108.4(1)	106.4(18), 108.0(15)
C3-C4-C11,C4-C3-C13	105.8(1)	107.3(12), 104.6(12)
C3-C13-C12,C4-C11-C12	106.2(1)	106.9(14), 106.2(12)
C3-C13-C14,C4-C11-C10	105.0(1)	104.7(20), 106.4(21)
C6-C7-C8	94.6(1)	94.1(20)
C8-C1-C14,C8-C9-C10	17.5(1)	116.5(14), 116.9(13)
C10-C11-C12,C12-C13-C14	111.2(1)	111.6(18), 108.9(15)
C11-C12-C13	102.3(1)	102.9(18)
O1-C10-C9,O2-C14-C1	125.3(1)	125.5(30), 125.0(30)
O1-C10-C11,O2-C14-C13	124.5(1)	125.0(30), 123.5(30)

[a,b)] As indicated in Table 3.

Table 5. Atomic coordinates and thermal parameters for non-hydrogen atoms of **21** with estimated standard deviations in parentheses

Atoms	X	Y	Z	B(iso),Å^2
O(1A)	0.1066(16)	0.0907(5)	0.3145(18)	5.2(6)
O(2A)	0.5595(18)	0.1559(5)	0.3503(18)	4.9(7)
O(1B)	1.4288(17)	0.1571(5)	1.0011(18)	4.5(6)
O(2B)	0.9708(16)	0.0960(5)	0.9569(18)	4.1(6)
C(1A)	0.6185(20)	0.0571(6)	0.3984(19)	3.0(6)
C(2A)	0.7105(20)	0.0062(7)	0.3582(19)	2.7(7)
C(3A)	0.6672(18)	0.0150(6)	0.2660(19)	2.9(7)
C(4A)	0.4662(19)	-0.0109(7)	0.2510(20)	3.0(7)
C(5A)	0.4001(20)	-0.0365(6)	0.3343(19)	3.5(7)
C(6A)	0.5757(23)	-0.0437(7)	0.3861(19)	3.7(8)
C(7A)	0.5081(23)	-0.0231(9)	0.4727(20)	3.8(8)
C(8A)	0.4333(22)	0.0360(7)	0.4351(18)	3.7(8)
C(9A)	0.2913(21)	0.0128(7)	0.3731(19)	3.4(7)
C(10A)	0.2303(20)	0.0536(7)	0.3090(20)	3.9(8)
C(11A)	0.3337(20)	0.0374(6)	0.2330(19)	3.0(6)
C(12A)	0.4628(20)	0.0882(6)	0.2016(19)	2.5(6)
C(13A)	0.6395(19)	0.0808(7)	0.2552(19)	3.4(7)
C(14A)	0.5981(21)	0.1048(7)	0.3366(19)	3.1(7)
C(1A′)	0.8135(19)	-0.0135(6)	0.2153(18)	2.9(7)
C(2A′)	0.9140(19)	-0.0647(7)	0.2348(18)	3.2(7)
C(3A′)	1.0357(22)	-0.0914(9)	0.1896(23)	4.9(10)
C(4A′)	1.060 (3)	-0.0713(10)	0.1063(21)	4.5(9)
C(5A′)	0.973 (3)	-0.0227(10)	0.0877(21)	4.7(10)
C(6A′)	0.8452(21)	0.0058(5)	0.1350(20)	3.4(7)
C(1B)	0.9210(20)	0.1919(6)	0.9068(20)	3.3(7)
C(2B)	0.8316(19)	0.2462(7)	0.9490(19)	3.0(7)
C(3B)	0.8661(19)	0.2360(7)	1.0410(18)	2.9(7)
C(4B)	1.0648(20)	0.2605(7)	1.0575(19)	2.6(7)
C(5B)	1.1405(20)	0.2855(6)	0.9791(19)	3.6(8)
C(6B)	0.9682(22)	0.2946(7)	0.9232(19)	3.1(7)
C(7B)	1.0409(22)	0.2737(9)	0.8469(20)	3.7(8)
C(8B)	1.1105(21)	0.2137(7)	0.8739(18)	3.8(8)
C(9B)	1.2525(20)	0.2366(7)	0.9400(20)	3.4(7)
C(10B)	1.3087(21)	0.1940(6)	1.0067(19)	3.0(7)
C(11B)	1.1938(20)	0.2085(7)	1.0822(19)	3.5(7)
C(12B)	1.0604(22)	0.1601(7)	1.1044(21)	4.0(8)
C(13B)	0.8872(19)	0.1692(6)	1.0553(19)	2.5(6)
C(14B)	0.9283(22)	0.1453(7)	0.9697(19)	3.5(8)
C(1B′)	0.7161(20)	0.2626(5)	1.0943(19)	2.6(6)
C(2B′)	0.6146(20)	0.3126(6)	1.0667(17)	3.2(7)
C(3B′)	0.4933(19)	0.3414(7)	1.1227(20)	2.5(7)
C(4B′)	0.4675(22)	0.3229(8)	1.1948(21)	3.8(8)
C(5B′)	0.5519(23)	0.2725(8)	1.2249(20)	3.9(9)
C(6B′)	0.6804(21)	0.2439(7)	1.1698(19)	3.6(8)

It should be noted that compound **4** exists in an equilibrium of two cyclooctane conformations: One defined as "boat-boat" (**4b**), that is also found in all remaining model compounds; the second, denoted as "chair-chair" (**4a**), being the predominant conformation as indicated by MNDO calculation ($\Delta H_f = -85.5$ vs. -75.0 kcal/mol).

In Table 1 results from semiempirical[18)] and ab initio[19)] calculations are compared with the experimental values. Predictions from MNDO and HAM/3 as well as from the STO-3G ab initio results are in good agreement with the experiment. It is not unusual[20)] that MNDO overestimates the absolute energies by about 1 eV, whereas STO-3G lowers them by 1 – 2 eV. But sequences and energetic splittings are reproduced rather satisfying.

Nevertheless no detailed information is given about the different ways of transmission via the σ skeleton. To interpret the spectral differences in our compounds we therefore use a procedure proposed by Heilbronner and Schmelzer (HS procedure)[21)] based on the STO-3G model.

This method first creates localized bond orbitals (LBO) by application of the distance criterium of Foster and Boys[22)]. The Hartree-Fock matrix in the basis of LBOs is a non-diagonal one; the diagonal elements provide the basis energies of the LBOs. The off-diagonal matix elements indicate the direct interaction parameters between the corresponding LBOs and thus give evidence about any through space interaction (OITS). With this procedure no OITS between the carbonyl lone pairs could be detected for compounds **1** – **4**. Even **5** and **6**, where the intercarbonyl distance and the directional angles seem to be well suited for OITS, the corresponding parameters are found to be zero. It should be noted, however, that only occupied orbitals are being delt with in the localization procedure. The LBO basis energies of the n_+ and n_- combination are (nearly) degenerate for all six model compounds. In order to explain the energetic split which is experimentally observed and theoretically predicted by the canonical MOs, mixing of the n orbitals with specified σ orbitals resulting in a different destabilization of HOMO and SHOMO energies is necessary.

To detect such relevant σ orbitals the LBOs are transformed into new symmetry-adapted, semi-localized MOs. With these as new basis in the HF matrix all non-diagonal elements in the rows and columns of the n orbital combi-

Table 6. Selected transannular distances in **1**–**6**

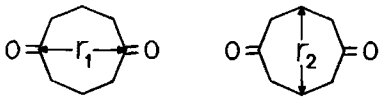

Compound	r_1[Å]	r_2[Å]
1	4.40	1.60
2	4.32	1.60
3	4.23	1.58
4	3.61	3.02
5	2.88	3.96
6	2.88	4.15

nations are set to zero. Subsequent diagonalization and transformation provides the socalled Precanonical MOs (PCMO) and, in addition, the corresponding HF matrix relating the PCMOs to the n orbitals.

In this matrix all non-diagonal elements of the n_+ and n_- combination showing an important coefficient indicate relevant PCMOs, which can now be subsequently mixed with the lone-pair combinations until the final situation of the canonical MOs is reproduced.

This was acomplished for compounds **1**–**6** as shown in Figure 4 for the two extreme topologies **1** and **6**. The relevant HF matrix elements of the corresponding PCMOs are given in Table 7.

As can readily be seen, from the application of the HS procedure to compounds **1**–**6** it is obvious that only a very small number of delocalized σ orbitals is necessary for efficient mixing: Thus in the case of **1** mixing of MO 51 with

Table 7. HF matrix elements of relevant PCMOs of **1**–**6**

1

MO	42	43	44(n_+)	45(n_-)	50	51
42	-12.63	0	0	-1.22	0	0
43	0	-11.81	2.53	0	0	0
44(n_+)	0	2.53	-11.80	0	1.15	0
45(n_-)	-1.22	0	0	-11.78	0	2.61
50	0	0	1.15	0	-10.13	0
51	0	0	0	2.61	0	-9.97

2

MO	37	40(n_+)	41(n_-)	43	46	48
37	-12.60	2.35	0	0	0	0
40(n_+)	2.35	-11.77	0	0	0	1.56
41(n_-)	0	0	-11.74	1.94	2.37	0
43	0	0	1.94	-11.17	0	0
46	0	0	2.37	0	-10.74	0
48	0	1.56	0	0	0	-10.31

3

MO	28	30	31	33(n_+)	34(n_-)	35
28	-13.60	0	0	2.57	0	0
30	0	-12.23	0	0	-1.95	0
31	0	0	-11.74	0	-2.52	0
33(n_+)	2.57	0	0	-11.58	0	1.00
34(n_-)	0	-1.95	-2.52	0	-11.54	0
35	0	0	0	1.00	0	-11.39

4

MO	30	32	35	36(n_-)	37(n_+)	38
30	-13.96	0	0	0	1.71	0
32	0	-12.71	0	-0.97	0	0
35	0	0	-11.55	-1.97	0	0
36(n_-)	0	-0.97	-1.97	-11.45	0	0
37(n_+)	1.71	0	0	0	-11.44	1.89
38	0	0	0	0	1.89	-11.29

5

MO	37	40	43	44(n_-)	45(n_+)	46
37	-13.00	0	0	0	1.39	0
40	0	-12.12	0	0	-0.60	0
43	0	0	-11.72	0	-1.76	0
44(n_-)	0	0	0	-11.64	0	-1.80
45(n_+)	1.39	-0.60	-1.76	0	-11.57	0
46	0	0	0	-1.80	0	-11.06

6

MO	44	46	51(n_-)	52(n_+)	53	54	56
44	-12.85	0	0	1.68	0	0	0
46	0	-12.12	0	-1.96	0	0	0
51(n_-)	0	0	-11.56	0	0	2.03	-1.33
52(n_+)	1.68	-1.96	0	-11.52	1.15	0	0
53	0	0	0	1.15	-11.40	0	0
54	0	0	2.03	0	0	-11.24	0
56	0	0	-1.33	0	0	0	-10.50

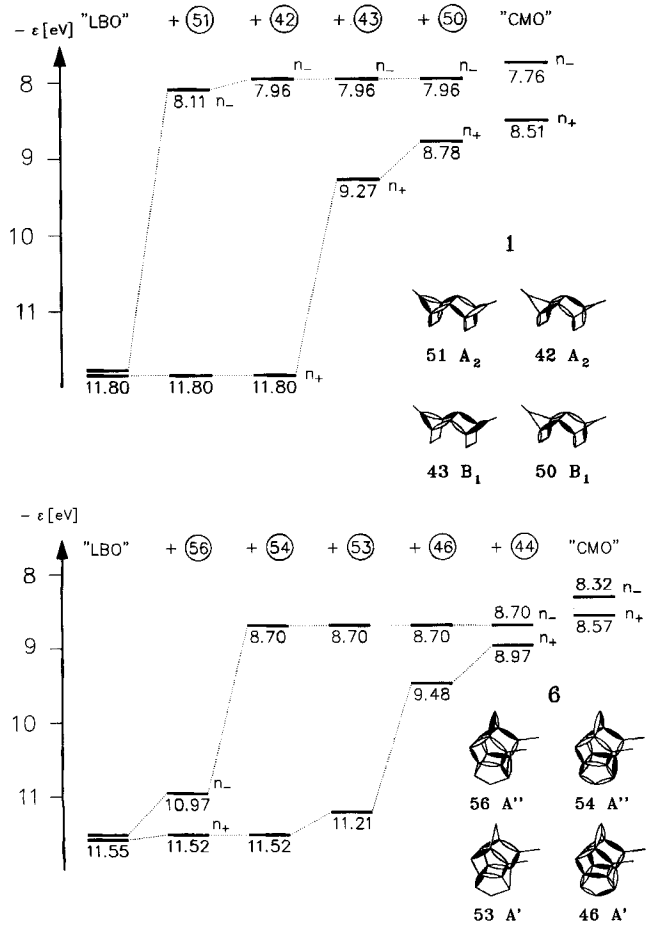

Figure 4. Mixing of localized n orbitals with relevant precanonical MOs of **1** and **6**

the n_- combination raises its basis energy by 3.67 eV; adding MO 42 results in an additional destabilization of only 0.15 eV. In contrast MOs 43 (+2.53 eV) and 50 (+0.53 eV) only mix with the n_+ orbital, resulting in a destibilization that is 0.84 eV smaller than that of the antisymmetrical combination. Due to the C_{2v} symmetry the latter is exclusively mixed with orbitals of the same irreducible representation A_2, whereas the former only combines with those of B_1. This result indicates that it is symmetry which determines the final splitting.

The splitting Δn = 0.75 eV observed in **1** to our knowledge is the largest one measured so far in a 1,5-diketone. The comparable compound **22** shows an even larger split (Δn = 0.94 eV)[23], it should, however, be classified as a 1,4-diketone with a shorter intervening σ pathway. Recently, a smaller split (Δn = 0.55 eV) has been found for 1,4-diketone **23**[24].

Scheme 9

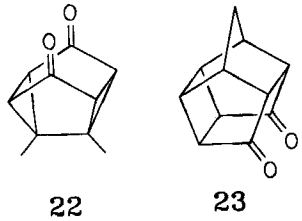

22 23

The unique and efficient σ skeleton in **1** owes its transmitting ability to both its zig-zag topology and its high energy of σ-PCMO 51 (−9.97 eV). It is mainly the interaction with that PCMO which determines the final remarkable split Δn = 0.75 eV.

Orbital interaction in birdcage **2** can be rationalized based on the same argument: Whereas the energy of the n_- combination is raised by MOs 46 (+2.93 eV) and 43 (+0.51 eV), both belonging to the irreducible representation A_2, the symmetrical n_+ orbital is less destabilized by mixing with MOs 37 (+1.97 eV) and 48 (+1.01 eV), both transforming as B_1. The resulting split between HOMO and SHOMO of 0.49 eV again is in good accordance with that of the canonical MOs calculated to 0.53 eV.

The PE spectrum of bicyclo[3.3.0]octane-3,7-dione (**3**) has previously been described[25]. The antisymmetrical lone-pair combination is destabilized by MOs of the corresponding irreducible representation A_2. A smaller destabilization is calculated for the n_+ orbital, which exclusevely combines with B_1 MOs. The final energetic difference of 0.66 eV approximately reproduces the splitting of the canonical MOs.

Showing the same C_{2v} symmetry as **1**, **2**, and **3**, compound **5** is readily analyzed with the help of the same arguments as above. Combination of the relevant A_2 MOs with the n_- and mixing of the corresponding B_1 MOs with the n_+ orbital results in an energetic split of 0.17 eV, which reproduces the canonical situation quite well.

In contrast to the preceeding model compounds cage dione **6** only exhibits C_s symmetry. But again it is this symmetry that determines combination of σ orbitals and lone-pair combinations. The split of the canonical MOs (0.25 eV) is excellently reproduced by mixing the n_- exclusively with the A″ MOs 56 (+0.55 eV) and 54 (+2.27 eV), whereas the n_+ orbital is combined with the A′ MOs 53 (+0.34 eV), 46 (+1.73 eV), and 44 (+0.51 eV). The resulting energetic difference is calculated to be 0.27 eV.

Finally, bicyclo[3.3.1]nonane-2,6-dione (**4**) is analyzed in its "chair-chair" conformation **4a**. Here symmetry is found to be C_2; and the n_+ combination is only mixed with the relevant MOs 35 and 32, both transforming as A, whereas the n_- orbital is combined with MOs 38 and 30, which can be assigned to B. The resulting split is in perfect accordance with the canonical MOs and gives a good explanation for the experimentally observed minimal splitting in the He(I_α) PE spectrum of **4**. As a result, the HS procedure provides good evidence about the individual participation of relevant precanonical molecular orbitals in OITB in compounds **1**–**6**. In addition, it indicates that the symmetry of lone-pair combination and corresponding (delocalized) σ orbital plays a determining role.

Photoreactivity

Inspection of Table 6 shows that only cage compound **6** is a possible condidate for transannular photoreactivity. In this case the nearly parallel alignment of the two carbonyl

groups and their short transannular distance seem to be well suited for Orbital Interaction Through Space (OITS). The LUMO of **6** consists of the symmetrical combination of π* orbitals of the carbonyl groups as shown in Scheme 10.

Scheme 10

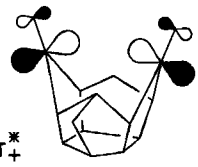

LUMO π_+^*

For an effective coupling reaction to happen it is necessary to promote an electron to the LUMO of **6**. This can be achieved either by metallic reduction to generate a radical anion or by direct (n,π*) photoexcitation. Without such a prerequisite the diol-forming reaction would not proceed in a favorable manner.

We thank Prof. Dr. *H. Musso*† (Institut für Organische Chemie der Universität Karlsruhe) for the generous gift of a sample of compound **4**. Financial support from the *National Science Council of the Republic of China* is gratefully acknowledged. TJC also appreciates a fellowship from the *Alexander von Humboldt-Stiftung* during the preparation of this manuscript. This work was also supported by the *Deutsche Forschungsgemeinschaft*, the *Fonds der Chemischen Industrie*, and the *BASF AG*.

Experimental

^{1}H and ^{13}C NMR: Bruker MSL-200 FT spectrometer. Chemical shifts of ^{1}H were measured downfield from tetramethylsilane in δ units, while those of ^{13}C were obtained using the central peak of $CDCl_3$ at δ 76.90 as an internal reference. – IR: Perkin-Elmer 297 infrared spectrophotometer. – Elemental analyses: Perkin-Elmer 240 EA instrument. – MS: Joel JMS-D300 mass spectrometer. – PE spectra: UPG-200, Leybold-Heraeus.

3,4,5,6-Tetrachloro-12,12-dimethoxy-endo,endo-tetracyclo-[6.2.1.1^{3,6}.0^{2,7}]dodeca-4,9-dien-11-ol: To a vigorously stirred suspension of 2.0 g (52.7 mmol) of $LiAlH_4$ in 150 ml of absol. THF a solution of 25.0 g (60.4 mmol) of **8** in 100 ml of the same solvent was added dropwise during 1 h. After 14 h at room temp. 200 ml of water was added cautiously followed by neutralization with dilute sulfuric acid until all precipitate was dissolved. THF was removed by distillation, and the aqueous phase was extracted with dichloromethane. After drying with $MgSO_4$ the solvent was distilled off to provide 19.85 g (88%) of a solid, which was recrystallized from methanol, m.p. 148°C. – IR (KBr): $\tilde{\nu}$ = 3300 (OH), 2950, 2840 (CH), 1600 cm^{-1} (C=C), 1445, 1375, 1320, 1290, 1255, 1180. – ^{1}H NMR ($CDCl_3$): δ = 2.37 (s, 1H), 3.3 (m, 2H), 3.12 (m, 2H), 3.50 (s, 3H), 3.62 (s, 3H), 3.97 (bs, 1H), 6.02 (m, 2H). – ^{13}C NMR ($CDCl_3$): δ = 48.9 (d, $^1J_{C,H}$ = 145 Hz), 49.0 (dq; $^1J_{C,H}$ = 150, $^3J_{C,H}$ = 7 Hz), 76.5 (s), 90.5 (d, $^1J_{C,H}$ = 153 Hz), 115.6 (s), 127.7 (s), 128.9 (d, $^1J_{C,H}$ = 172 Hz). – MS (70 eV): *m/z* (%) = 370 (0.5) [M$^+$], 335 (13) [M – Cl], 253 (100), 207 (22).

$C_{14}H_{14}Cl_4O_3$ (372.1) Calcd. C 45.19 H 3.79
Found C 45.40 H 3.86

3,4,5,6-Tetrachloro-12,12-dimethoxy-endo,endo-tetracyclo-[6.2.1.1^{3,6}.0^{2,7}]dodec-4-en-11-ol (**10**): 1.0 g (2.69 mmol) of the above alcohol was dissolved in 20 ml of $CHCl_3/CH_3OH$ (1:1, v/v). 50 mg of palladium (5%) on charcoal was added, and the mixture was submitted to hydrogenation at normal pressure. After the calculated amount of hydrogen was consumed the reaction mixture was filtered. The filtrate on evaporation afforded **10** (0.97 g, quant.) as colorless crystals, m.p. 162°C. – IR (KBr): $\tilde{\nu}$ = 3200 cm^{-1} (OH), 3000, 2960, 2940, 2830 (CH), 1595 (C=C), 1440, 1355, 1310, 1280, 1170, 1075. – ^{1}H NMR ($CDCl_3$): δ = 1.63 (m, 4H), 1.77 (s, 1H), 2.35 (m, 2H), 2.89 (t, 2H), 3.53 (s, 3H), 3.6, (s, 3H), 4.10 (m, 1H). – ^{13}C NMR ($CDCl_3$): δ = 21.1 (t, $^1J_{C,H}$ = 134 Hz), 42.5 (dd; $^1J_{C,H}$ = 145, $^3J_{C,H}$ = 7 Hz), 51.4, 52.7 (2 q, $^1J_{C,H}$ = 147 Hz), 76.6 (s), 80.7 (d, $^1J_{C,H}$ = 152 Hz), 118.1 (s), 129.4 (s). – MS (70 eV): *m/z* (%) = 336 (100) [M$^+$ – Cl].

$C_{14}H_{16}Cl_4O_3$ (374.1) Calcd. C 44.95 H 4.31
Found C 44.79 H 4.22

12,12-Dimethoxy-endo,endo-tetracyclo[6.2.1.1^{3,6}.0^{2,7}]dodec-4-en-11-ol: To 10.0 g (26.7 mmol) of alcohol **10** in 200 ml of absol. THF 6.0 g (261 mmol) of finely cut sodium in 100 ml of liquid ammonia was slowly added through a cooled (dry ice) dropping funnel. Addition was stopped when discolorization of the deep blue drops could not be observed any longer. Then the reation was interrupted by carefully adding solid NH_4Cl. After the remaining ammonia was completely evaporated within ca. 12 h 100 ml of water was added, and most of the tetrahydrofuran was removed by distillation. Upon extraction of the aqueous phase with chloroform, drying with $MgSO_4$, and evaporation a yellow solid remained. Chromatography (silica gel; ethyl acetate) afforded 3.45 g (55%) of colorless crystals, m.p. 125°C. – IR (KBr): $\tilde{\nu}$ = 3460 cm^{-1} (OH), 2950, 2835 (CH), 1465, 1440, 1330, 1265, 1155. – ^{1}H-NMR ($CDCl_3$): δ = 1.32 (m, 4H), 1.83 (s, 1H), 2.07 (m, 2H), 2.40 (m, 2H), 2.80 (m, 2H), 3.12 (s, 3H), 3.17 (s, 3H), 4.00 (m, 1H), 6.08 (t, 2H). – ^{13}C NMR ($CDCl_3$): δ = 22.9 (t, $^1J_{C,H}$ = 133 Hz), 40.9 (d, $^1J_{C,H}$ = 140 Hz), 44.1 (dd; $^1J_{C,H}$ = 142, $^3J_{C,H}$ = 6.5 Hz), 47.0 (dq; $^1J_{C,H}$ = 145, $^3J_{C,H}$ = 6.5 Hz), 49.6, 51.9 (2 q, $^1J_{C,H}$ = 142 Hz), 82.5 (d, $^1J_{C,H}$ = 150 Hz), 123.0 (s), 128.9 (d, $^1J_{C,H}$ = 170 Hz). – MS (70 eV): *m/z* (%) = 236 (27) [M$^+$], 221 (5) [M – CH_3], 205 (14) [M – OCH_3], 189 (1), 153 (14), 152 (40), 150 (53), 75 (100).

$C_{14}H_{20}O_3$ (236.3) Calcd. C 71.16 H 8.53
Found C 70.92 H 8.46

12,12-Dimethoxy-endo,endo-tetracyclo[6.2.1.1^{3,6}.0^{2,7}]dodecan-11-ol (**12**): A mixture of 6.4 g (213 mmol) of hydrazine hydrate and 0.5 ml of a 2% $CuSO_4$ solution was added to 1.00 g (4.23 mmol) of the above alcohol, dissolved in 12 ml of EtOH. After cooling to 5°C 20 ml of 30% H_2O_2 was added dropwise until formation of gases (oxygen and nitrogen) stopped. The reaction mixture was then poured onto 100 ml of water. After extraction with *n*-pentane the organic phase was washed with dilute hydrochloric acid and water before drying with $MgSO_4$. On evaporation of the solvent colorless needles began to crystallize yielding 0.53 g (52%) of **12**, m.p. 124°C. – IR (KBr): $\tilde{\nu}$ = 3300 cm^{-1} (OH), 2950, 2830 (CH), 1315, 1295, 1260, 1195, 1175, 1140, 1080, 1055. – ^{1}H NMR ($CDCl_3$): δ = 1.78 (m, 4H), 2.20 (m, 6H), 2.35 (s, 1H), 3.23 (s, 6H), 4.06 (s, 1H). – ^{13}C NMR ($CDCl_3$): δ = 22.0, 22.4 (2 t, $^1J_{C,H}$ = 134 Hz), 38.9 (d, $^1J_{C,H}$ = 132 Hz), 41.6 (d, $^1J_{C,H}$ = 142 Hz), 45.4 (dd; $^1J_{C,H}$ = 141, $^3J_{C,H}$ = 6 Hz), 50.0, 50.5 (2 q, $^1J_{C,H}$ = 142 Hz), 82.8 (dt; $^1J_{C,H}$ = 151, $^3J_{C,H}$ = 6 Hz), 116.8 (s). – MS (70 eV): *m/z* (%) = 238 (19) [M$^+$], 153 (50), 124 (23), 101 (100).

$C_{14}H_{22}O_3$ (238.3) Calcd. C 70.56 H 9.30
Found C 70.38 H 8.95

12,12-Dimethoxy-endo,endo-tetracyclo[6.2.1^{3,6}.0^{2,7}]dodecan-11-one: To a suspension of 5.00 g (50 mmol) of CrO_3 in 300 ml of dry dichloromethane 8.00 g (101 mmol of pyridine was added dropwise with vigorous stirring. After 30 min all CrO_3 had dissolved. To this

mixture 0.85 g (357 mmol) of **12** in 20 ml of dichloromethane was added at one time. After 0.5 the organic phase was decanted and washed twice with concd. Na_2CO_3 solution, dilute hydrochloric acid, and water. After drying with $MgSO_4$ the mixture was filtered through a silicagel column with elution with further dichloromethane. On evaporation the ketone (0.61 g, 72%) crystallized as a colorless rhombic solid, m.p. 108°C. – IR (KBr): $\tilde{\nu}$ = 3025 cm^{-1}, 2980, 2920, 2890 (CH), 1755 (CO), 1480, 1445, 1285, 1245, 1175, 1090. – ^1H NMR ($CDCl_3$): δ = 1.60–2.70 (m, 14H), 3.25 (s, 3H), 3.28 (s, 3H). – ^{13}C NMR ($CDCl_3$): δ = 18.9 (t, $^1J_{C,H}$ = 137 Hz), 22.4 (t, $^1J_{C,H}$ = 135 Hz), 34.5 (d, $^1J_{C,H}$ = 136 Hz), 42.0 (d, $^1J_{C,H}$ = 143 Hz), 44.3 (d, $^1J_{C,H}$ = 150 Hz), 50.2, 50.5 (2 q, $^1J_{C,H}$ = 142 Hz), 115.1 (s), 211.2 (s). – MS (70 eV): *m/z* (%) = 236 (4) [M^+], 208 (3) [M – CO], 205 (4) [M – OCH_3], 153 (100).

$C_{14}H_{20}O_3$ (236.3) Calcd. C 71.16 H 8.25
Found C 70.36 H 8.53

endo,endo-Tetracyclo[6.2.1.1^{3,6}.0^{2,7}]dodeca-11,12-dione (**1**): 0.30 g (1.27 mmol) of the above ketone, dissolved in 12.5 ml of THF, was mixed with 7.5 ml of 6 M $HClO_4$. After 3 h the reaction mixture was poured onto ice/water, extracted with dichloromethane and the organic phase dried with $MgSO_4$. On evaporation a white solid remained which was recrystallized from chloroform to afford **1** (0.18 g, 74%), m.p. 161.5°C. – IR (KBr): $\tilde{\nu}$ = 3040 cm^{-1}, 3010, 2975, 2930, 2885 (CH), 1720 (CO), 1490, 1450, 1365, 1265, 1230, 1145. – ^1H NMR ($CDCl_3$): δ = 1.60–2.80 (m). – ^{13}C NMR ($CDCl_3$): δ = 19.0 (t, $^1J_{C,H}$ = 137 Hz), 30.8 (bd, $^1J_{C,H}$ = 136 Hz), 43.3 (d, $^1J_{C,H}$ = 150 Hz), 210.0 (s). – MS (70 eV): *m/z* (%) = 190 (95) [M^+], 162 (16) [M – CO], 134 (12) [M – 2CO], 107 (71), 91 (100).

$C_2H_{14}O_2$ (190.2) Calcd. C 75.76 H 7.42
Found C 76.15 H 7.36

Photolysis of **6** *in 2-Propanol:* Into a quartz vessel (5 ml), fitted with a gas inlet, were given 2-propanol (2 ml) and **6** (31.2 mg, 0.146 mmol). The resulting mixture was deoxygenated by irradiating with ultrasound while purging with nitrogen gas for 30 min. The solution was then irradiated with a Hanovia 450 watt medium pressure mercury lamp for another 30 min. The diol **13** was collected upon evaporating 2-propanol and was purified by recrystallization (31.0 mg, 0.144 mmol, 98%). – The ^1H, ^{13}C NMR, and mass spectra of **13** have been reported in a preliminary communication[8].

$C_{14}H_{16}O_2$ (214.3) Calcd. C 77.74 H 7.45
Found C 77.52 H 7.34

Zinc Reduction of **6**: Into a round bottom flask (10 ml), containing a magnetic stirring bar, were given **6** (12 mg, 0.056 mmol), zinc powder (30 mg, 0.46 mmol), and acetic acid (3 ml). The resulting mixture was stirred at room temp. for 30 min. It was then poured into ice/water, neutralized with 5% sodium hydroxide solution, and was extracted three times with chloroform. The combined organic solution was dried with $MgSO_4$ and concentrated in vacuo. The diol **13** was collected in 95% yield (11.5 mg, 0.052 mmol).

Photolysis of **6** in THF: Into a quartz vessel (10 ml), containing a magnetic stirring bar, were filled **6** (72 mg, 0.34 mmol) and freshly distilled THF (3 ml). The resulting solution was degassed as previously described and irradiated with UV light for 4 h. It was concentrated in vacuo while **13** crystallized (8.0 mg, 0.037 mmol, 11%). The oily fraction was applied to a silica gel chromatographic column that was eluted with hexane/ethyl acetate (3:2, v/v). The mono-THF adduct **15** (58 mg, 0.020 mmol, 60%) and the bis-THF adduct **16** (25 mg, 0.070 mmol, 21%) were collected as colorless oils. The ^{13}C-NMR and mass spectra of **15** have been reported previously[5]. – ^1H NMR ($CDCl_3$): δ = 1.70 (m, 7H), 1.92 (d, *J* = 10 Hz, 1H), 2.20 (OH), 2.35 (m, 1H), 2.42 (m, 6H), 2.51 (m, 2H), 2.64 (m, 1H), 3.58 (t, *J* = 6 Hz, 2H), 5.00 (t, *J* = 4 Hz, 1H).

$C_{18}H_{22}O_3$ (286.4) Calcd. C 74.54 H 7.80
Found C 74.04 H 7.74

High resolution MS: Calcd. 286.1569, Found 286.1545

Compound **16** appears as a mixture of diastereomers, its ^{13}C-NMR, mass, and IR spectra have been reported previously. – ^1H NMR ($CDCl_3$): δ = 1.65–2.00 (m, 12H), 2.38 (m, 1H), 2.45 (m, 6H), 2.53 (m, 2H), 2.66 (m, 1H), 3.35 (m, 1H), 3.65 (m, 1H), 3.80 (m, 2H), 5.02 (m, 1H), 5.07 (m, 1H).

$C_{22}H_{28}O_4$ (356.5) Calcd. C 73.71 H 8.43
Found C 73.59 H 7.94

Photolysis of **6** *in the Presence of Benzophenone:* Into a quartz vessel (25 ml) were given **6** (103 mg, 0.48 mmol), benzophenone (170 mg, 0.93 mmol), and benzene (20 ml). The solution was degassed as before and was irradiated with UV light for 14 h. After evaporating the solvent, the products were separated by passing through a silica gel column eluted with hexane/ethyl acetate (4:1, v/v). The phenyl adduct **21** was collected (23 mg, 0.079 mmol, 75% corrected yield) along with the unreacted starting materials (80 mg). – ^1H NMR ($CDCl_3$): δ = 1.94 (s, 2H), 2.44–2.50 (m, 1H), 2.74–2.82 (m, 3H), 2.92–3.03 (m, 3H), 3.12–3.20 (m, 2H), 3.39–3.47 (m, 2H), 7.22–7.37 (m, 5H). – ^{13}C NMR ($CDCl_3$): δ = 42.99 (d), 43.79 (t), 47.17 (t), 48.16 (d), 55.07 (d), 55.66 (d), 56.24 (d), 56.97 (d), 57.81 (d), 62.63 (d), 63.14 (d), 68.56 (s), 124.86 (d), 126.22 (d), 128.83 (d), 147.82 (s), 221.76 (s). – MS (70 eV): *m/z* (%) = 290 (100) [M^+], 262 (8) [M^+ – CO], 234 (2.8) [M^+ – 2CO], 196(30).

High resolution MS: $C_{20}H_{18}O_2$ Calcd. 290.1307
Found 290.1303

Photolysis of **7** *in the Presence of Benzophenone:* Into a quartz vessel (25 ml), fitted with a gas inlet, were given the cage compound **7** (1.05 g, 5.69 mmol), benzophenone (1.04 g, 5.90 mmol), and benzene (20 ml). The solution was degassed, then was irradiated with UV light for 18 h. The products were separated by eluting through a silica gel column with hexane/ethyl acetate (20:1, v/v). The phenyl adduct **20** was collected (304 mg, 1.17 mmol, 47% corrected yield) along with the starting material (587 mg). – ^1H NMR ($CDCl_3$): δ = 1.78–1.97 (m, 4H), 2.04–2.65 (m, 9H), 2.77 (s, 1H), 2.89–2.92 (d, *J* = 4 Hz, 1H), 7.13–7.17 (m, 1H), 7.23–7.34 (m, 4H). – ^{13}C NMR ($CDCl_3$): δ = 42.05 (t), 42.64 (t), 51.21 (d), 51.41, (d), 51.92 (d), 52.05 (d), 52.98 (d), 53.38 (d), 53.69 (d), 54.51 (d), 62.16 (d), 62.35 (d), 67.85 (s), 124.90 (d), 125.88 (d), 127.94 (d), 148.57 (s). – MS (70 eV): *m/z* (%) = 260 (100) [M^+], 183 (0.7) [M^+ – Ph], 91 (16).

$C_{20}H_{20}$ (260.4) Calcd. C 92.26 H 7.74
Found C 92.18 H 8.13

X-Ray Diffraction Analyses of **6** *and* **21**: A single crystal of **6** grown to the size of 0.15 mm × 0.50 mm × 0.50 mm was subjected to a Nonius CAD-4 automated diffractometer using monochromated (graphite) Mo-K_α radiation (λ = 0.70930 Å, μ = 0.09 mm^{-1}, *F*(000) = 455.95). The Θ/2Θ scan method was employed with minimum 2Θ = 3° and maximum 2Θ = 49.8°. The reciprocal lattice segment was found to be: a^* = 0.1496; b^* = 0.0803; c^* = 0.0180; α^* = 90.0016; β^* = 89.8571; γ^* = 90.0235. The crystal is orthorhombic, *Pbc*2_1, *a* = 6.684 (14), *b* = 12.451(7), *c* = 12.353(12) Å, *V* = 1028.10 $Å^3$, *Z* = 4, and *D* = 1.384 g/cm^3. Out of 948 unique reflections, 876 were found to have intensity $I > 2.5\sigma(I)$ and were used as observations in the crystal structural solution and refinements (direct method of solution, full matrix). All computations were carried out on a VAX 780 computer with an NRCC package. At full convergence the agreement factors are *R* = 0.061 and R_w = 0.072 for significant reflections, and in the difference map the min-

imum and maximum are −0.20 and 0.48 e/Å^3. The final atomic fractional coordinates and temperature factors, bond lengths and angles are listed in the supplementary materials[26].

The crystal structure of **21** was elucidated similarly. A crystal of 0.15 mm × 0.20 mm × 0.65 mm was subjected to a Nonius CAD-4 diffractometer with monochromated (graphite) Mo-K_α radiation (λ = 0.7093 Å, μ = 0.08 mm^{-1}, $F(000)$ = 1231.86). The intensity data were collected using the $\Theta/2\Theta$ scan mode with minimum $2\Theta = 3°$ and maximum $2\Theta = 49.8°$. The reciprocal lattice segment is found to be: $a^* = 0.14291$; $b^* = 0.04311$; $c^* = 0.05947$; $\alpha^* = 90.0339$; $\beta^* = 89.9714$; $\gamma^* = 89.9728$. The crystal is orthorhombic, $Pbc2_1$, a = 6.997(3), b = 23.198(6), c = 16.816(4) Å, V = 2729.46 Å^3, Z = 8, and D = 1.413 g/cm^{-3}. The number of unique reflections measured were 2485, among which 1224 were found to have intensity greater than $2.5\sigma(I)$ and were used for structure refinements. All data reduction and refinement (direct method of solution, full matrix) were performed by means of the NRCC-SDP-VAX package. At full convergence, the agreement factors are R = 0.061 and R_w = 0.072 for significant reflections, and in the final difference map the minimum and maximum are found to be −0.200 and 0.480 e/Å^3. The unit cell contains asymmetrical molecules, their final atomic coordinates and temperature factors, bond lengths and angles are listed in the supplementary materials[26].

CAS Registry Numbers

1: 131213-98-4 / **2**: 98230-14-9 / **3**: 131213-99-5 / **4**: 16473-11-3 / **6**: 112533-27-4 / **8**: 131320-22-4 / **10**: 131214-00-1 / **12**: 131214-01-2 / **13**: 122860-93-9 / **15**: 131235-84-2 / **16**: 122860-94-0 / **20**: 131235-85-3 / **21**: 131214-02-3 / 12,12-dimethoxy-*endo,endo*-tetracyclo[6.2.1^{3,6}.0^{2,7}]dodecan-11-one: 131214-03-4

---

[1] Dedicated to Professor *Horst Prinzbach* on the occasion of his 60th birthday.
Part 74: H. J. Altenbach, D. Constant, H.-D. Martin, B. Mayer, M. Müller, E. Vogel, *Chem. Ber.* **124** (1991) 791, preceding.

[2] [2a] R. Hoffmann, *Acc. Chem. Res.* **4** (1971) 1. – [2b] H. D. Martin, B. Mayer, *Angew. Chem.* **95** (1983) 281; *Angew. Chem. Int. Ed. Engl.* **22** (1983) 283. – [2c] R. Gleiter, *Angew. Chem.* **86** (1974) 770; *Angew. Chem. Int. Ed. Engl.* **13** (1974) 696. – [2d] M. N. Padden-Row, *Acc. Chem. Res.* **15** (1982) 245.
[3] T. Koopmans, *Physica* **1** (1934) 104.
[4] H.-D. Martin, B. Albert, H.-J. Schiwek, *Tetrahedron Lett.* **1979**, 2347.
[5] Compound **5** was not available for PE experiments; synthesis is described in: [5a] P. Engel., J. W. Fischer, L. A. Paquette, *Z. Kristallogr.* **166** (1984) 225. – [5b] L. A. Paquette, A. R. Browne, C. W. Doecke, R. V. Williams, *J. Am. Chem. Soc.* **105** (1983) 4113. – [5c] L. A. Paquette, J. W. Fischer, A. R. Browne, C. W. Doecke, *J. Am. Chem. Soc.* **107** (1985) 686.
[6] [6a] G. Schroeter, *Liebigs Ann. Chem.* **426** (1922) 1. – [6b] S. H. Bertz, G. Rihs, R. B. Woodward, *Tetrahedron* **38** (1982) 63.
[7] [7a] H. Meerwein, W. Schürmann, *Liebigs Ann. Chem.* **398** (1913) 196. – [7b] A sample of **4** was generously provided by Prof. Dr. H. Musso† (Institut für Organische Chemie der Universität Karlsruhe).
[8] T. J. Chow, T.-K. Wu, *J. Org. Chem.* **53** (1988) 1102.
[9] [9a] T. J. Chow, Y.-S. Chao, L.-K. Liu, *J. Am. Chem. Soc.* **109** (1987) 797. – [9b] A. P. Marchand, A. D. Earlywine, *J. Org. Chem.* **49** (1984) 1660. – [9c] T. J. Barden, M. N. Paddon-Row, *Aust. J. Chem.* **41** (1985) 817.
[10] [10a] B. Franzus, W. C. Baird Jr., E. J. Snyder, J. H. Surridge, *J. Org. Chem.* **32** (1967) 2945. – [10b] P. R. Story, S. R. Fahrenholtz, *J. Am. Chem. Soc.* **87** (1965) 1623. – [10c] P. R. Story, S. R. Fahrenholtz, *J. Am. Chem. Soc.* **86** (1964) 1270.
[11] H. Prinzbach, G. Sedelmeier, W.-D. Fessner, R. Pinkos, C. Grund, B. A. R. C. Murty, D. Hunkler, G. Rihs, H. Fritz, C. Krüger, *Chem. Ber.* **119** (1986) 3442.
[12] H. Prinzbach, J. P. Melder, F. Wahl, *Chimia* **41** (1987) 426.
[13] E. J. Corey, W. L. Mock, D. J. Pasto, *Tetrahedron Lett.* **1961**, 347. – [13b] S. Hünig, H. R. Müller, W. Thier, *Tetrahedron Lett.* **1961**, 353.
[14] [14a] E. Wenkert, J. E. Yoder, *J. Org. Chem.* **35** (1970) 2896. – [14b] J. E. McMurry, J. G. Rico, *Tetrahedron Lett.* **30** (1989) 1169.
[15] T. J. Chow, T.-K. Wu, *Tetrahedron Lett.* **30** (1989) 1279.
[16] [16a] T. Mori, K H. Yang, K. Kimoto, H. Nozaki, *Tetrahedron Lett.* **1970**, 2419. – [16b] W. T. Borden, T. Ravindranathan, *J. Org. Chem.* **36** (1971) 4125. – [16c] R. Bishop, *Aust. J. Chem.* **36** (1983) 2465. – [16d] T. Sasaki, S. Eguchi, T. Kiriyama, O. Hiroaki, *Tetrahedron* **30** (1974) 2707. – [16e] B. Föhlisch, U. Dukek, I. Graessle, B. Novotny, E. Schupp, G. Schwaiger, E. Widmann, *Liebigs Ann. Chem.* **1973**, 183.
[17] [17a] H. Setter, J. Gärtner, P. Tacke, *Chem. Ber.* **98** (1965) 3888. – [17b] K.-W. Shen, N. A. Keubler, *Tetrahedron Lett.* **1973**, 2145. – [17c] R. Bishop, *J. Chem. Soc., Perkin Trans. 1* **1974**, 2364. – [17d] R. R. Sauers, A. Scimone, H. Shams, *J. Org. Chem.* **53** (1988) 6084.
[18] [18a] M. J. S. Dewar, W. Thiel, *J. Am. Chem. Soc.* **99** (1975) 4899. – [18b] R. C. Bingham, M. J. S. Dewar, D. H. Lo, *J. Am. Chem. Soc.* **97** (1975) 1285. – [18c] L. Asbrink, C. F. Fridh, E. Lindholm, *Chem. Phys. Lett.* **52** (1977) 69.
[19] W. J. Hehre, R. F. Stewart, J. A. Pople, *J. Chem. Phys.* **51** (1969) 2657.
[20] H.-D. Martin, B. Mayer, R. W. Hoffmann, A. Riemann, P. Rademacher, *Chem. Ber.* **118** (1985) 2514.
[21] [21a] E. Heilbronner, A. Schmelzer, *Helv. Chim. Acta* **58** (1975) 936. – [21b] G. Bieri, E. Heilbronner, A. Schmelzer, *Helv. Chim. Acta* **60** (1977) 2234.
[22] [22a] J. M. Foster, S. F. Boys, *Rev. Mod. Phys.* **32** (1969) 300. – [22b] M. Scholz, H. J. Köhler, *Quantenchemie*, vol. 3, p. 384, Dr. Alfred Hüthig Verlag, Heidelberg 1981. – [22c] D. Peeters, QCPE-Program Nr. 330, QCPE *Newsletters* **57** (1977) 19.
[23] G. Jähne, R. Gleiter, *Angew. Chem.* **95** (1983) 500; *Angew. Chem. Int. Ed. Engl.* **22** (1983) 488.
[24] A. P. Marchand, C. Huang, R. Kaya, A. D. Baker, E. D. Jemmis, D. A. Dixon, *J. Am. Soc.* **109** (1987) 7095.
[25] S. P. McGlynn, D. Dougherty, P. Brint, *J. Am. Chem. Soc.* **100** (1978) 5597.
[26] Further details of the crystal structure investigations are available on request from the Fachinformationszentrum Karlsruhe, Gesellschaft für wissenschaftlich-technische Information mbH, D-7514 Eggenstein-Leopoldshafen 2, on quoting the depository number CSD-54922, the names of the authors, and the journal citation.

[268/90]